PCCP

Accepted Manuscript

ROYAL SOCIETY OF CHEMISTRY

www.rsc.org/pccp

Cite this: DOI: 10.1039/c0xx00000x

www.rsc.org/xxxxxx

PAPER

Fabrication of collagen scaffolds impregnated with sago starch capped silver nanoparticles suitable for biomedical applications and its physicochemical studies†

Abhishek Mandal,[a,b] Santhanam Sekar,[b] Kamal Mohamed Seeni Meera,[c] Amitava Mukherjee,[a] Thotapalli P. Sastry,*[b] Asit Baran Mandal,*[b,c,d]

Received (in XXX, XXX) Xth XXXXXXXXX 20XX, Accepted Xth XXXXXXXXX 20XX
DOI: 10.1039/b000000x

Present investigation attempts at fabricating collagen-based scaffolds impregnated with sago starch capped silver nanoparticles (AgNPs), useful for biomedical applications and aims at studying its physicochemical aspects. AgNPs synthesized through chemical reduction method, capped using different concentrations of sago starch are incorporated into collagen derived from fish scales, and lyophilized to form scaffolds. FT-IR spectra confirm and validate the interaction of sago starch capped AgNPs with collagen in the scaffolds. TGA and DSC results indicate enhanced thermal stability of collagen scaffolds impregnated with sago capped AgNPs compared to collagen alone. All the collagen scaffolds containing sago starch capped AgNPs show high tensile strength values for their use as wound dressing material. Moreover, lower minimum inhibitory concentration values obtained for the above capped AgNPs collagen scaffolds, which indicate higher antibacterial activities compared to uncapped AgNPs tested against both gram positive and negative bacterial strains. Novelty is that the developed scaffolds are biodegradable and *in vitro* studies reveal them as biocompatible and suitable for tissue regeneration applications.

1. Introduction

Nanomaterials as biomaterials have gained significant use in various biomedical applications.[1] The controllable syntheses of nanostructures particularly silver nanoparticles (AgNPs) play prominent roles in fabricating nanoscale devices with special electronic, transport, optical, and mechanical properties on confinement and have received wide attention.[2] Moreover, the use of AgNPs as antimicrobial agent[3,4] has been widely recognized and applied in different medical fields such as for ocular applications,[5] sustained drug delivery,[6,7] surgical catheters,[8] and dressing of infected wounds.[9-12]

It has been widely reported that the silver nanoparticles specifically imparted their antimicrobial activity by interacting the disulfide bonds of the glycoprotein or altering the protein structure of the microorganism such as bacteria and fungi, thereby blocked its functional operations. i.e., it exerted an oligodynamic action by exhibiting either bactericidal or bacteriostatic impact.[13,14] Thus, AgNPs acted as a potent antibacterial agent that demonstrated strong cytotoxicity by annihilating the bacterial cell membranes and could be applied in biomedical research.[15,16]

Both synthetic and natural polymers have been used extensively as capping agent to prevent the aggregation and thus provide added stability to the nanoparticles. Sago starch, a well-known carbohydrate polymer, is one of the most abundant and inexpensive polysaccharides, which has unique properties such as superior biodegradability and biocompatibility.[17-19] In addition to the above mentioned properties, the scaffolds prepared from sago starch satisfy the requirement of adequate thermal stability and minimum interference with flow properties essential for biomedical applications.[20] Thus, encapsulation of silver nanoparticles by starch can be employed in developing scaffolds for biomedical purposes. However, the application of scaffolds developed from starch is limited due to water absorption and poor mechanical properties.[21,22] In order to overcome these limitations, the addition of another polymer to improve the properties is required.[23]

[a]*Centre for Nano-Biotechnology, School of Bio-Sciences and Technology, VIT University, Vellore 632014, India.*
[b]*Bio-Products Laboratory, Council of Scientific and Industrial Research (CSIR)-Central Leather Research Institute (CLRI), Adyar, Chennai 600020, India.*
[c]*Polymer Division, CSIR-CLRI, Adyar, Chennai 600020, India.*
[d]*Chemical Laboratory, CSIR-CLRI, Adyar, Chennai 600020, India.*
**Email: abmandal@hotmail.com, abmandal@clri.res.in (A. B. Mandal), sastrytp@hotmail.com (T. P. Sastry)*
Fax #: +91-44-24912150/24911589; Tel #: +91-44-24910846/24910897
†Electronic Supplementary Information (ESI) available: [FT-IR, Particle size, SDS-PAGE, Zeta potential, MIC, DSC, TGA, and porosity data]. See DOI: 10.1039/b000000x/

Collagen, another biopolymer, is an insoluble fibrous protein found abundantly in the extracellular matrix and connective tissues of mammals.[24] Type I collagen extracted from bovine source is mainly used in medical applications but concerns related to transmissible disease such as bovine spongiform encephalopathy observed in these collagen products has led to the search for alternative sources of collagen.[25,26] Therefore, a number of alternative sources such as chrome leather waste,[27] chicken skin,[28] and different marine animals like squid,[29] octopus,[30] starfish,[31] swim bladder of catfish,[32,33] and so forth have been attempted. Among them, fish source is relatively safe and thus collagen derived from its wastes (scales) provides as an alternate option. Hence, collagen extracted from different fish scales, both fresh water as well as marine water have been used for biomedical applications.[34,35] The scales of marine sources are cheaper and more abundant than that of the fresh water origin. However, one of the problems associated with collagen derived from marine fish scales is its relatively low denaturation temperature that limits its biomedical applications significantly.[36-38] As a result, we have chosen to extract collagen from fish scales of marine origin and develop scaffolds that have biomedical applications. The association of silver nanoparticles with biopolymers such as sago starch and collagen offers an attractive approach in developing biomaterials with potential biomedical applications. Very recently, preparation and characterization of aloe vera blended collagen-chitosan composite scaffold for tissue engineering applications was reported by us.[39] To the best of our knowledge, no reports on the capping of silver nanoparticles by sago starch and their interactions with fish scale collagen have been documented.

Therefore, the objectives of this study are to design, synthesize and characterize the collagen scaffolds derived from marine fish origin impregnated with more stable silver nanoparticles capped by different concentrations (1, 2 and 3µM) of sago starch, which would have potential biomedical applications especially, in wound healing process. The role of capped AgNPs on the physicochemical properties of the prepared scaffolds was investigated using various physicochemical techniques. Moreover, the antibacterial activity of these scaffolds was tested against both gram negative and positive bacterial strains. Furthermore, the viability of these scaffolds on fibroblast NIH 3T3 cell lines was also investigated. The schematic representation of the fabrication and characterization of biocompatible collagen scaffolds impregnated with sago starch capped silver nanoparticles is shown in Fig. S1.

2. Experimental section

2.1. Materials

Fish scales of *Lates Calcarifer* were collected from nearby fish market. Also, sago starch (MW 20 $\times 10^6$) was purchased from nearby local retail market. Silver nitrate ($AgNO_3$) and sodium borohydride ($NaBH_4$) were purchased from Sigma-Aldrich, St. Louis, Mo, USA. Bacterial strain, Escherichia coli (*E. coli*) was obtained from the microbiology department, Central Leather Research Institute, Chennai, India. Muller Hinton medium was purchased from Hi-media laboratories Pvt. Ltd, Mumbai, India. All the chemicals and reagents used were of analytical grade and purchased from Sigma–Aldrich. Deionized water with a specific conductance of 2 µS cm^{-1} at 25°C was used throughout the work.

2.2. Methods

UV–vis measurements were made on a Jasco Spectrophotometer Model UV-VIS-V530 and photoluminescence spectrum was obtained on Hitachi F-2500. Fourier-transform infrared (FT-IR) spectroscopic analysis was carried out using Perkin-Elmer Spectrum 2000 instrument and scanning electron microscopy (SEM) was done on Philips XL-30. The TEM analyses for the sago starch coated NPs were carried out using Tecnai10 Philips transmission electron microscope and the images were captured using a voltage of 80 kV. The thermal analyses (TGA and DSC) of the scaffolds were conducted on a Perkin-Elmer Model No. 7. The particle size analysis along with their zeta potential was confirmed using Malvern instruments (Zetasizer 3000 HS_A). Mechanical properties of the scaffolds at an extension rate of 5 mm/min were assessed with INSTRON model (1405 SATRA, UK, Model No. TM-43) at 20 °C.

2.3. Extraction of fish scale collagen (FSC)

The isolation of collagen from fish scales of *Lates Calcarifer* was performed using a modified method reported earlier.[40] In brief; fish scales were washed with running water to remove sand and other foreign bodies and later exposed under sunlight. 500 g of dried fish scales were soaked in 10% H_2SO_4 solution for 24 h. The fish scales were then minced by using a mincer. The resultant fine paste was subjected to centrifugation (12,000 rpm) at 4ºC for 20 min. This supernatant was collected and its pH was adjusted to 7 using calcium hydroxide solution. The supernatant solution was further centrifuged at 10,000 rpm for 15 min to remove calcium sulfate salts. The supernatant had collagen solids (60%) and was stored at 4ºC.

2.4. Synthesis of silver nanoparticles (AgNPs)

The experiment was carried out in a dark room at 4 ºC. To 1 mL of $AgNO_3$ (0.01 M) solution, 5 mL of $NaBH_4$ (0.02 M) solution was added drop wise with continuous stirring for 20 min. The appearance of pale yellow color indicates the generation of silver nanoparticles in the solution.

2.5. Synthesis of sago starch capped silver nanoparticles (SGAgNPs)

Sago was sieved and powdered using a domestic mixer. 2, 4 and 6 g of sago starch were dissolved in 100 mL milliQ water and boiled to obtain the concentrations of 1, 2 and 3 µM, respectively. The contents were added to 1 mL of $AgNO_3$ (0.01 M) solution. 5 mL of $NaBH_4$ (0.02 M) solution was added drop wise with continuous stirring for 20 min to ensure the completion of the reaction. The above experiment was carried in a dark cold room at 4 ºC.

2.6. Preparation of FSC scaffolds impregnated with sago starch capped AgNPs (FSC-SG-AgNPs)

To the beaker containing 10 mL of the fish scale collagen solution, 10 mL of silver nanoparticles solution added with continuous stirring by the magnetic stirrer. The process of stirring was carried out for 15 min. The contents were poured in a petri-dish and subjected to lyophilization to obtain scaffolds in the form of sponges. The concentration of silver nanoparticle

(AgNPs) used in the fabrication of scaffolds which has been kept at ~90 µM.

2.7. SDS-PAGE

The confirmation of collagen derived from fish scales were performed *via* SDS-PAGE following Laemmli's[41] method. A gel (8%) was prepared and the films were dissolved in SDS sample buffer solution containing 1% SDS, 1% mercaptoethanol, 20% glycerol and heated for 5 min at 100 °C. The films were subjected to gel electrophoresis at a constant current of 2V/cm. After electrophoresis, the gels were stained with 0.1% (w/v) Coomassie Brilliant Blue R-250 and the gel images were captured on a BIOVIS gel documentation system.

2.8. Minimum inhibitory concentration (MIC)

In order to determine the antibacterial properties of all the scaffolds represented as FSC, FSC-AgNPs, FSC-SG1-AgNPs, FSC-SG2-AgNPs and FSC-SG3-AgNPs, the minimum inhibitory concentrations (MIC) of the above scaffolds were determined by following the standard procedures provided below.[42] To the pre-sterilized Muller Hinton broth solution, test samples of concentrations ranging from 0.002-2 mg were added individually. The test cultures viz., *Staphylococcus aureus* (ATTC 29213) and *Escherichia coli* (ATTC 25922) chosen for the present investigation are grown in nutrient broth separately and 50 µL (1 x10^3) of 18 h grown cultures are inoculated, where the final absorbance of the test solution maintained at 0.5. The samples along with respective blanks (culture and broth alone) are incubated for 24 h at 37 °C. Followed by incubation, the turbidity of the growth medium is monitored at 600 nm and the reduction in colony forming units (CFU) is determined using spread plate technique. The solution keeping the absorbance fixed at 0.05 turns turbid at a particular concentration, which was considered as the MIC of the sample and all the experiments were conducted in triplicate.

2.9. Cell viability, attachment and proliferation studies

Mice fibroblasts (NIH 3T3) were cultured in DMEM with 10% FBS and 1% antibiotic-antimycotic at humified atmosphere of CO_2 (5%) and 37 °C. The medium was replenished every 3 days. For *in vitro studies*, the scaffold was cut into 1x1 cm and placed into the wells on a 24 well plate individually. Before seeding cells, scaffolds were sterilized by immersion in 70% ethanol for 2 h, washed 3 times with PBS, and then washed with culture medium. Cells were then seeded at a density (10^5) cells/well of 24-well plates and tissue culture polystyrene (TCP) wells were seeded as control. The viability of NIH 3T3 cells on collagen based scaffolds after 24 and 48 h of seeding were determined by methylthiazol tetrazolium (MTT) assay. The attachment and proliferation of NIH 3T3 cells on the scaffolds was evaluated using fluorescent microscope. Regarding details of the cell morphology, compatibility and cytotoxicity of the prepared scaffolds, we have described in our recent publication.[39]

2.10. Statistical analysis

Cell adhesion and proliferation experiments were performed in triplicate and the data were presented as mean ± standard deviation (SD). The results were compared by one-way analysis of variance (ANOVA) followed by Duncan multiple comparison test using SPSS 13 software. All the values of $p < 0.05$ were considered statistically significant.

3. Results and discussion

3.1. UV-vis spectra

The UV-vis spectra (Fig. 1) show peak characteristic of the silver surface plasmon resonance (SPR) at around 400 nm, which indicates the generation of AgNPs. This characteristic peak was further shifted to 403, 405 and 408 nm for silver nanoparticles capped by 1, 2 and 3 µM concentrations of sago starch, respectively. Moreover, sharp and intense peaks indicate the formation of nano-sized silver particles.[43,44] The particle sizes of the sago starch coated AgNPs were determined by the particle size analyzer (PSA). The AgNPs capped by 1 µM sago starch were found to be in the range of 30-60 nm in comparison to 40-90 nm for the uncapped AgNPs. Moreover, the AgNPs capped by 2 and 3 µM sago starch, as illustrated in Fig. S2 were found to be in the range of 20-45 nm and 15-40 nm, respectively. This shows that the size of silver nanoparticles reduced with the increase in the concentration of sago starch capping agent.

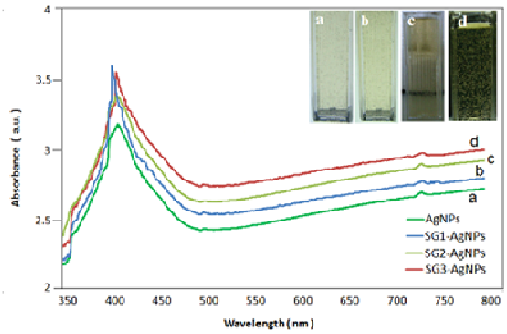

Fig. 1 UV-Vis spectra of silver nanoparticles uncapped (a) and capped by (b) 1 µM, (c) 2 µM, and (d) 3 µM sago starch, respectively.

3.2. Zeta potential

The zeta potential measurements were performed to assess the stability of the synthesized silver nanoparticles, which is essential for the development of biomaterial applications.[45] The measured zeta potential values of the silver nanoparticles are depicted in Table S1. The value of -15±0.5 mV suggests that the uncapped silver nanoparticles were stable with time. For 1, 2 and 3 µM sago starch capped silver nanoparticles, the zeta potential values were found to be -20.1±0.8, -21.4 ±0.6 and -23.3±0.5 mV, respectively. The low zeta potential values suggest that the capped nanoparticles are more stable due to steric repulsion. This is attributed to the fact that sago starch acts as a stabilizer and restricts the mobility of the silver ions and thereby avoids agglomeration in the course of the reaction. The hydrophilic chains of the starch molecule containing –OH groups, which forms strong association with AgNPs and prevent aggregation leading to the formation of more nano-sized and stable silver particles.[46]

3.3. SDS-PAGE

The isolation of collagen from the scales of *Lates Calcarifer*, a marine fish, was confirmed with the SDS-PAGE. The SDS-PAGE has been used to determine the purity and elucidate the type of collagen. The results of the SDS-PAGE are shown in Fig.

S3 reveal three distinct bands assigned to the β, α_1 and α_2, respectively. The two α bands (α_1 and α_2) noticed at 116 and 97.4 KDa are attributed to the unfolding polypeptide chains of collagen triple helix.[40,41] Thus, the observed characteristic bands confirm the triple helicity of the type I collagen.

3.4. ATR-FTIR spectra

The ATR-FTIR spectroscopy was used to understand the interaction of sago starch capped AgNPs with collagen. The ATR-FTIR spectroscopic data for FSC-AgNPs and different concentrations of sago starch encapsulated AgNPs in collagen scaffolds at 20 °C are depicted in Table S2. The effect of different concentrations of sago starch on the encapsulation of AgNPs in collagen scaffolds were studied in the present investigation and illustrated in Fig. S4. It was found that the peak at 3240 cm^{-1} due to –OH group contribution of the collagen moiety was shifted to 3261 cm^{-1} upon interaction with AgNPs. This characteristic peak was further shifted to higher region *viz.*, 3289, 3296 and 3291 cm^{-1} in collagen scaffolds when the concentrations of sago starch were 1, 2 and 3 µM, respectively. This is due to the fact that sago starch exhibits a broad band from 3100-3600 cm^{-1} attributed to the vibration of –OH group present in the molecule. In addition to this, other characteristic peaks of sago starch were observed in the finger print regions *viz.*, 1075 and 950 cm^{-1} respectively. Moreover, the broad peak noticed at 1646 cm^{-1} is due to the presence of tightly held bound water in the starch and the band at 2925 cm^{-1} represents the C–H stretching vibration. The shift in the peaks is observed with the increase in starch concentration and this effect is most probably due to the encapsulation of sago starch on the silver nanoparticles. The FT-IR spectra of all these scaffolds show the characteristic bands of both collagen and starch, however, shifting of the bands in the fingerprint region from 950 to 1075 cm^{-1} and 1425 to 1420 cm^{-1} are observed. This may be due to the interaction between –OH groups of starch and NH_2 groups of collagen. Also, peaks at 1652 cm^{-1} (amide I C=O stretching), 1552 cm^{-1} (amide II N–H stretching) and the peaks in the range 1143-1301 cm^{-1} due to amide III (contributions from C–N stretching and N–H stretching) were observed.[47] Furthermore, the value of transmittance ratio (T_{1454}/T_{1234}) calculated was found to be close to unity (1) in all the scaffolds, which indicated that the triple helical structure of collagen remained intact and not perturbed by sago starch.[48] This also validates the chemical interaction between sago starch and collagen present in the scaffolds.

3.5. Thermal studies

The denaturation temperature of fish scale collagen determined from the DSC curve was found to be 38 °C (Fig. 2). In the above DSC curve, we also observed three more peaks at 91, 121 and 225 °C and they are associated with the water loss owing to dehydration. We designate these three melting peaks as $T_m(1)$, $T_m(2)$ and $T_m(3)$, respectively (see Table S3). The water losses in the temperature ranges around 40-80 °C and 80-200 °C obtained from TGA curves are due to free water and bound water losses, respectively (Fig. 3). The charring and carbon formations are generally occurred in the systems at temperatures above 200 °C, which is not required in the present context. The results obtained from DSC and TGA are given in Tables S3 and S4, respectively.

It has been noticed from Table S4 that the free water loss was significantly reduced when collagen is capped with AgNPs (in the temperature region 20-80 °C) compared to its un-capped state. However, the opposite trend was observed with regard to bound water loss (in the temperature range 80-200 °C). TGA results also indicate that the loss of free water increase in the collagen scaffolds with the increase in concentration of the starch used for capping AgNPs than that in absence of starch (Table S4), whereas the opposite trend was observed with regard to bound water loss. These are quite interesting observations.

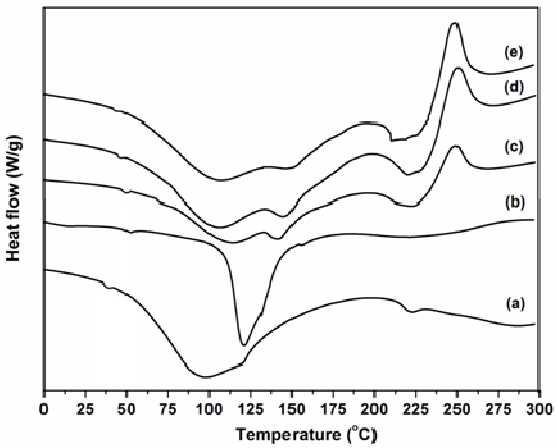

Fig. 2 DSC curves of prepared collagen and collagen-based scaffolds: (a) collagen; (b) FSC-AgNPs; (c) FSC-SG1-AgNPs; (d) FSC-SG2-AgNPs; and (e) FSC-SG3-AgNPs, respectively.

The DSC results indicate that the denaturation temperature (T_d) of collagen alone is 38 °C. The T_d of the above collagen is enhanced to 52 °C when it is incorporated with AgNPs. However, the T_d values of the collagen scaffolds were found to be 48, 45 and 43 °C in the presence of AgNPs capped by 1, 2 and 3 µM starch, respectively. With regard to melting peaks $T_m(1)$, $T_m(2)$ and $T_m(3)$, these values are enhanced to 121, 156 and 227 °C in AgNPs capped collagen from 91, 123 and 225 °C respectively, which are obtained in collagen alone. The above melting temperature $T_m(1)$ decreases with the increase of starch concentration. However, with regard to $T_m(2)$ and $T_m(3)$, there is not much change observed. The above results suggest that the biodegradability of the collagen in AgNPs is possible in presence of starch with its optimum concentration. Therefore, it is worthwhile to discuss the above biodegradable phenomenon in light of some thermodynamic parameter, which is as follows:

The activation energy, E_a associated with the process was calculated using the following equation:[49,50]

$$ln\left(ln\frac{Q_t}{Q_t - Q}\right) = \frac{E_a}{R}\left(\frac{1}{T_m} - \frac{1}{T}\right) \quad (1)$$

Where, Q_t and Q are the total heat of the process and heat evolved, respectively at a given temperature. T_m is the temperature at the endotherm, whereas R is the universal gas constant (8.314 $JK^{-1}mol^{-1}$). Q_t and Q are determined from the area under the endotherm. A plot of $ln[ln\{Q_t/(Q_t\text{-}Q)\}$ versus 1/T has given a straight line (see Fig. S5), whose slope is $-E_a/R$. The E_a values along with correlation coefficient are depicted in Table S3.

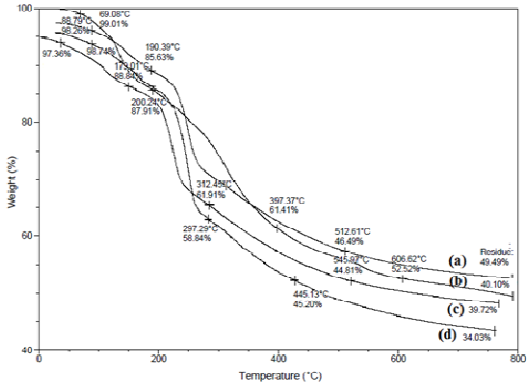

Fig. 3 TGA traces of prepared collagen-based scaffolds: (a) FSC-AgNPs; (b) FSC-SG1-AgNPs; (c) FSC-SG2-AgNPs; and (d) FSC-SG3-AgNPs, respectively.

3.6. Water absorption and porosity studies

The water absorption studies were conducted to determine the biodegradability of the prepared scaffolds. Since, hydrolysis is the prime mechanism that governs the degradation of polymer in the human body, the study of water uptake is essential for the polymeric tissue engineered scaffolds and their potential applications.[51] The water uptake of the prepared scaffolds was calculated using the following formula:[52]

$$\text{Water uptake } (\%) = \frac{(W_o - W_i)}{W_i} \times 100 \quad (2)$$

Where W_i and W_o are the initial dry and observed wet weights of the scaffold at different time interval (t), respectively.

The porosities of the prepared scaffolds were also determined from the procedure followed by Shimizu *et al.*[53] are given in Table S5. Percent porosity was calculated using the following equation:

$$\text{Porosity } (\%) = \left[1 - \frac{(W_w - W_d)}{SV}\right] \times 100 \quad (3)$$

Where SV is scaffold volume; W_w and W_d are the wet and initial dry weights of the scaffolds, respectively.

It is important to determine the water absorption capacity (WAC), as scaffolds with better WAC when applied on an open wound surface can easily absorb wound exudates and ensure that the wounds are dry and in turn avoids air borne infections.[54] All the scaffolds in the present study exhibited increased water absorption capacity with increase in time and the maximum capacity attained at 24 h (See Fig. S6). Also, it can be noted that the water absorption capacity increases with the increase in the sago concentration and the maximum value was observed in FSC-SG3-AgNPs in comparison to the other scaffolds. This could be attributed to the fact that sago starch contains hydroxyl groups on its polysaccharide backbone, which are hydrophilic in nature and thus, leads to increased water absorption. Moreover, it is well understood that a porous scaffold can take up and store more water compared to the non-porous scaffolds.[51] As the concentration of starch increases from 1 to 3 µM in collagen scaffolds, it results in higher porosity due to larger pore sizes and thus has more space for water storage. With the increase in collagen content, the functional groups such as, $–NH_2$ and –COOH present in collagen weakly interacts with the hydroxyl groups of sago starch and thus reduces the hydrophilicity of the FSC-SG1-AgNPs scaffold as well as the water absorption capacity.[55] Therefore, FSC-SG3-AgNPs scaffold shows the highest ratio of water absorption and thus exhibits maximum swelling among the scaffolds. The results indicate that the prepared scaffolds are biodegradable and possess the capacity to absorb water suitable for tissue engineering applications, especially in wound dressing biomaterials preparations.

3.7. Mechanical properties

Recent research is focused on developing wound dressing materials with improved mechanical properties so that it can be applied on to wound properly.[56] The mechanical properties of the scaffolds are given in Table 1. Tensile strength, the mechanical property required for biomedical applications such as clinical wound healing was the least in the case of sago starch film (10.1 MPa) and highest with a value of 24.3 MPa in the case of FSC-AgNPs scaffold respectively. However, significant increase in tensile strength was observed in the case of FSC-SG1-AgNPs. This increased value of 19.5 MPa for the biodegradable scaffold is attributed to the formation of intermolecular hydrogen bonding between NH_4^+ of the collagen backbone and OH^- of the sago starch. Furthermore, with increase in the concentration of sago starch in FSC-SG2-AgNPs and FSC-SG3-AgNPs, a decrease in the tensile strength was noticed. This decrease in tensile strength is most probably due to the increased crystallinity of starch in the scaffolds. Also, the value of elongation at break (E) was affected by the increase in sago starch concentration. Accordingly, with the increase in content of sago starch, the diffusion rate of water increased and subsequently, the percentage elongation of the scaffolds decreased. The Young's Modulus values in the case of collagen based scaffolds containing impregnated starch capped silver nanoparticles were found to be higher with the increase in sago starch concentration. However, the increase of Young's Modulus is due to the presence of sago starch, which was maximum (953 MPa) in the case of FSC-SG2-AgNPs. With further increase in starch content in FSC-SG3-AgNPs, the value of Young's modulus (649.3 MPa) decreased. The increase in the elasticity of the FSC-SG2AgNPs scaffold could be useful and find potential in the preparation of heart valves.

Table 1: Mechanical Properties of sago starch, uncapped silver nanoparticles and different concentration of sago starch capped silver nanoparticles impregnated in fish scale collagen scaffolds (FSC) at 20 °C with 65% relative humidity.

Scaffold Composition	Elongation at break (%)	Young's Modulus (MPa)	Tensile Strength (MPa)
Sago Starch (SG)	8.31± 0.71	490 ± 17.3	10.1 ± 0.68
FSC-AgNPs	32.8± 2.4	116.19 ± 22.41	24.3 ± 1.25
FSC-SG1-AgNPs	7.88± 0.5	598.47±12.6	19.5 ± 0.94
FSC-SG2-AgNPs	6.83± 0.3	953.16 ±18.23	15.5 ± 0.58
FSC-SG3-AgNPs	5.12± 0.4	649.29 ± 15.42	13.4 ± 0.67

3.8. SEM/EDX and TEM of the prepared scaffolds

The surface morphology of the prepared scaffolds analyzed by using SEM is depicted in Fig. 4. The SEM images reveal the homogenous and uniform distribution of silver nanoparticles in the collagen scaffolds. The impregnation of sago starch capped silver nanoparticles onto collagen matrix has led to more smooth surface, which is essential and a pre-requisite of a material to be

used as wound dressing purposes. Also, it was observed that the collagen scaffolds were found to be more porous with the increase in the sago starch concentration used in the capping of AgNPs. The presence of interconnected pores satisfies the requirement for its use as scaffolds for biomaterial applications. The EDX spectrum exhibits a strong signal of silver atoms, which confirms the presence of silver nanoparticles in the collagen scaffolds. The additional signals of C and O atoms noticed in the collagen scaffold are attributed to the carbon moieties and carboxyl groups present in the collagen. The higher intensity of carbon and oxygen signals observed in the scaffolds containing capped silver AgNPs is due to the presence of carbon moieties and hydroxyl groups of sago starch used to encapsulate the silver nanoparticles.

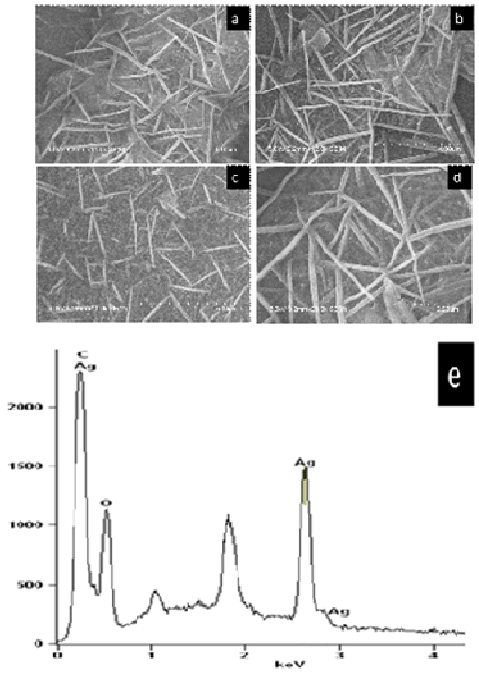

Fig. 4 SEM images of the collagen based scaffolds: (a) FSC-AgNPs; (b) FSC-SG1-AgNPs; (c) FSC-SG2-AgNPs; (d) FSC-SG3-AgNPs; and (e) EDX profile of FSC-SG3-AgNPs.

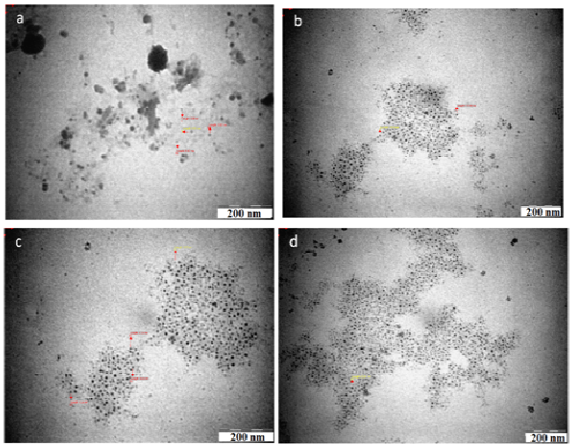

Fig. 5 TEM images of the collagen based scaffolds: (a) FSC-AgNPs; (b) FSC-SG1-AgNPs; (c) FSC-SG2-AgNPs; and (d) FSC-SG3-AgNPs, respectively.

Furthermore, the TEM images also confirm the homogenous distribution of sago starch encapsulated AgNPs on to the collagen matrix (See Fig. 5), as observed in the SEM. The size of these capped AgNPs were found to reduce with the increase in the concentration of the capping agent, sago starch from 1 to 3 µM and was found to be 30, 20 and 16 nm, respectively. This corroborates with the findings from PSA and authenticates the formation of nanoparticles and their reduction in size with the increase in sago starch concentrations.

3.9. Cytotoxicity studies

The minimum inhibitory concentrations (MICs) for fish scale collagen (FSC) and AgNPs impregnated collagen scaffolds in absence and presence of starch tested against both gram positive and negative bacterial strains are depicted in Fig. S7. The sago starch capped AgNPs show lower MIC value compared to the collagen scaffolds impregnated with uncapped AgNPs. The above MIC values for FSC alone are 400±15 and 520±20 µg/mL for *E. coli* and *S. aureus*; whereas for uncapped FSC-AgNPs are 295±18 and 480±28 µg/mL for *E. coli* and *S. aureus*, respectively. In the recent past, we have found[57] that the critical micelle concentration (CMC) of the anti depressant hydantoin drug is more or less equal to MIC. However, Moulik *et al.*[58] have recently observed that the MIC values are two to three times lower than those of CMCs for some normal and reverse Pluronics viz., PEO-PPO-PEO and PPO-PEO-PPO. We had first investigated that the sepia cartilage collagen formed micelles[59] whose CMC value was found to be 300 µg/mL at 20 °C. However, the CMC value of the above collagen[59] was largely depended on temperature and nature of additive environments with geometry changes.[33,59] In the present investigation, we have not correlated between MIC and CMC of FSC; a separate study will be made in detail in future. Moreover, the MIC values of AgNPs reported by Chudasama *et al.*[60] in the recent past were found to be 100 and 300 µg/mL for *E. coli*. and *S. aureus*, respectively. There is no report available for MIC values of SG to the best of our knowledge. Furthermore, it has been observed that MIC values decrease with increase in sago starch concentration. Thus, FSC-SG3-AgNPs exhibit a value of 205±12 µg/mL lower than 213±15 and 238±13 µg/mL for FSC-SG2-AgNPs and FSC-SG1-AgNPs respectively for *E. coli*. Similarly, for gram positive bacterial strain, *S. aureus*, lower value of 390±25 µg/mL was noted in the case of FSC-SG3-AgNPs in comparison to 410±23 and 440±21 µg/mL for FSC-SG2-AgNPs and FSC-SG1-AgNPs, respectively. These findings are probably due to penetrations of stable silver particles, which have smaller sizes. In addition, lower MIC values were observed in the case of *E. coli*, the gram negative bacteria compared to *S. aureus*, the gram positive bacterial strain. This is due to the fact that the gram negative bacteria do not have a cell membrane and therefore, silver nanoparticles can easily react with cellular contents of the bacteria.[61] It can be concluded that the smaller sized AgNPs capped by sago starch probably diffused more easily than the uncapped larger AgNPs, which explains the higher toxicity observed on the bacterial strains used in this study. Therefore, AgNPs capped by sago starch provide enhanced antibacterial property to the collagen scaffolds prepared for potential biomedical applications such as material for wound dressings.

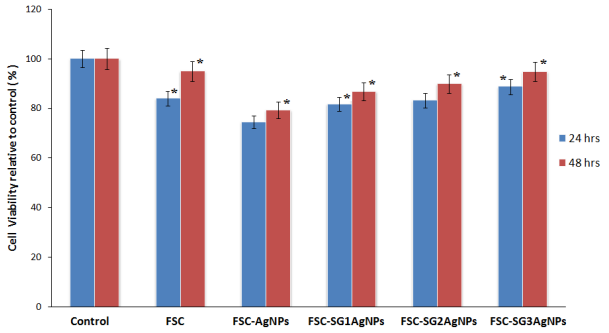

Fig. 6 Cell viability of fibroblast (NIH 3T3) cells cultured on FSC, FSC-AgNPs; FSC-SG1-AgNPs; FSC-SG2-AgNPs; and FSC-SG3-AgNPs relative to control (TCP) at time periods of 24 and 48 h respectively. The asterisks (*) indicate statistically significant differences compared to the control ($p < 0.05$).

The results of the cytotoxicity effects on fibroblast (NIH 3T3) cells cultured on the collagen based scaffolds are depicted in Fig. 6. The viabilities of NIH 3T3 cells expressed as the absorbance value obtained at 540 nm for the developed scaffolds show good cytocompatibility in comparison with tissue culture plate used as control. The viability of fibroblast (NIH 3T3) cells on bare FSC scaffold was found to be 84% at 24h and increases to 94% after 48h, respectively. The addition of uncapped AgNPs on to collagen scaffold reduced the viability (75% and 79% at 24 and 48 h, respectively) of the fibroblasts. However, it was noted that with increase in the concentration of starch (1-3 µM) capped silver nanoparticles impregnated on the collagen scaffolds exhibited an increase in the cell viability from 81 to 89% at 24 h, respectively. Similar trend of higher cell viability (85-94%) after 48 h in all the collagen based scaffolds containing starch capped AgNPs was observed. According to the observations of our study, the concentrations of starch (1-3µM) capped AgNPs used are seemingly within the safety limit, as it did not cause much cell death in NIH 3T3 culture even after 48 h time period. Thus, starch capped AgNPs impregnated on collagen scaffolds could be safely employed in tissue engineering applications, as they possess cytocompatibility along with antibacterial activity.

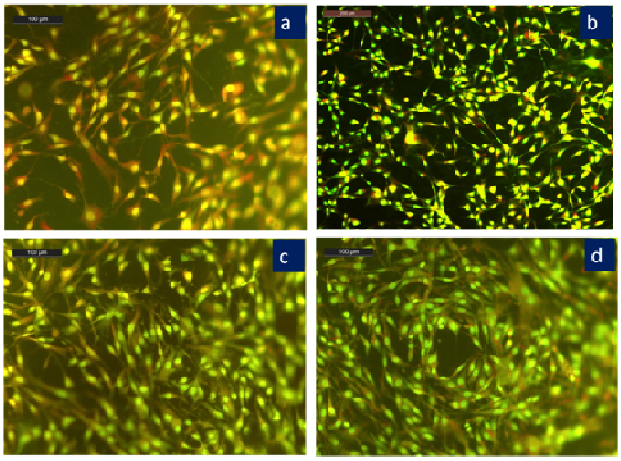

Fig. 7 Fluorescence micrographs (20X) of fibroblast cells after 48 h of culture on (a) FSC-AgNPs; (b) FSC-SG1-AgNPs; (c) FSC-SG2-AgNPs; and (d) FSC-SG3-AgNPs scaffolds, respectively.

The morphology of the NIH 3T3 cells adhered on the collagen scaffolds impregnated with starch capped AgNPs was assessed through fluorescence microscopy, as shown in Fig. 7. The fibroblast cells proliferated rapidly and became confluent at 48 h. As these collagen based scaffolds derived from fish scales of marine origin have an interconnected and highly porous structure, NIH 3T3 cells were well distributed on the scaffolds. Also, it was noticed that the cells anchored to the nano fibrous architecture of the collagen based scaffolds accumulated and oriented in the direction of fibers resulting in a well spread-out morphology. Furthermore, cellular extensions and protrusions due to contact between the individual cells were observed. This finding may be attributed to the high affinity of NIH 3T3 cells to collagen and their migration around the scaffolds.[36] Moreover, it has been demonstrated that the presence of silver nanoparticles modulates the alignment of collagen and augment the fibroblast cell proliferation and its differentiation.[62] Here, in our case, the *in vitro* results suggest that the starch capped silver nanoparticles impregnated in the collagen scaffolds perform this function, which is vital for clinical wound healing application.

4. Conclusions

In the present study, a novel biomaterial from natural resources *viz.*, fish scales and sago starch for various biomedical applications was developed. Stable silver nanoparticles (AgNPs) capped by different sago starch concentrations (1, 2 and 3 µM) were successfully synthesized using green approach. These nanoparticles were incorporated into collagen extracted from fish scales, lyophilized to form scaffolds with enhanced stability, which was confirmed by TGA and activation energies obtained from DSC. The above scaffolds also show enhanced antibacterial efficacy on both gram positive and negative bacterial strains in comparison to collagen scaffolds with uncapped silver nanoparticles. Though the tensile strength of the scaffolds decreased with the increase in sago starch concentration, the values indicate that the prepared scaffolds could be used as wound dressing material. Moreover, improved Young's Modulus values were observed for collagen scaffolds containing sago starch capped silver nanoparticles, which suggest that the combinations of these biopolymers increase the elasticity and these scaffolds could find use in the preparation of synthetic heart valves. The *in vitro* studies show that the prepared scaffolds are biocompatible, where the capped silver nanoparticles provide strong antibacterial property to the scaffolds and can be used for tissue engineering applications. Overall, the present study provides a clear picture about the physicochemical and biological properties of the prepared novel collagen scaffolds.

Acknowledgements

The Council of Scientific and Industrial Research (CSIR), Ministry of Science and Technology, Government of India, New Delhi is gratefully acknowledged for the support of this research work. Authors also acknowledge Dr. C. Rose and Mr. P. Jithendra, Dept. of Biotechnology, CSIR-CLRI, for their technical help in fluorescence microscopic measurements.

References

1 (a) C. Blanco-Andujar, L. D. Tung and N. T. K. Thanh, *Annu. Rep. Prog. Chem. Sect. A*, 2010, **106**, 553–568; (b) A. C. Schneid, E. W. Roesch, F. Sperb, U. Matte, N. P. da Silveira, T. M. H. Costa, E. V. Benvenutti and E. W. de Menezes, *J. Mater. Chem. B*, 2014, **2**, 1079–1086; (c) K. Seeni Meera, R. Murali Sankar, J. Paul, S. N. Jaisankar and A. B. Mandal, *Phys. Chem. Chem. Phys.*, 2014, **16**, 9276–9288.

2 W. Gang, L. Wang, Z. Liu, Y. Song, L. Sun, T. Yang and Z. Li, *J. Phys. Chem. B*, 2005, **109**, 23941–23947.

3 M. Rai, A. Yadav and A. Gade, *Biotechnol. Adv.*, 2009, **27**, 76–83.

4 M. Mahmoudi and V. Serpooshan, *ACS Nano, 2012, **6***, 2656–2664.

5 C. M. Santoro, N. L. Duchsherer and D. W. Grainger, *Nanobiotechnol.*, 2007, 3, 55–65.

6 P. Sujatha, S. Balaji, T. P. Sastry and A. B. Mandal, *J. Biomed. Nanotechnol.*, 2008, **4**, 62–66.

7 N. Shanmugasundaram, J. Sundaraseelan, S. Uma and M. Babu, *J. Biomed. Mater. Res. B Appl. Biomater.*, 2006, **77B**, 378–388.

8 D. Roe, B. Karandikar, N. Bonn-Savage, B. Gibbins and J. Roullet, *J. Antimicrob. Chemother.*, 2008, **61**, 869–876.

9 P. Rujitanaroj, N. Pimpha and P. Supaphol, *Polymer*, 2008, **49**, 4723–4732.

10 K. Varaprasad, Y. M. Mohan, K. Vimala and K. M. Raju, *J. Appl. Polym. Sci.*, 2011, **121**, 784–796.

11 M. P. Arockianathan, S. Sekar, S. Sankar, B. Kumaran and T. P. Sastry, *Carbohydr. Polym.*, 2012, **90**, 717–724.

12 P. T. S. Kumar, Abhilash, K. Manzoor, S. V. Nair, H. Tamura and R. Jayakumar, *Carbohydr. Polym.*, 2010, **80**, 761–767.

13 W. K. Jung, H. C. Koo, K. W. Kim, S. Shin, S. H. Kim and Y. H. Park, *Appl. Environ. Microbiol.*, 2008, **74**, 2171–2178.

14 S. Agnihotri, S. Mukherji and S. Mukherji, *Nanoscale*, 2013, **5**, 7328–7340.

15 H. H. Lara, E. N. Garza-Treviño, L. Ixtepan-Turrent and D. K. Singh, *J. Nanobiotechnol.*, 2011, **9**, 2–8.

16 T. Maneerung, S. Tokura and R. Rujiravanit, *Carbohydr. Polym.*, 2008, **72**, 43–51.

17 V. Ramnath, S. Sekar, S. Sankar and T. P. Sastry, *Int. J. Pharm. Bio. Sci.*, 2011, **1**, 577–585.

18 18. S. Mali and M. V. E. Grosmann, *J. Agric. Food Chem.*, 2003, **51**, 7005–7011.

19 F. B. Ahmad, P. A. Williams, J. Doublier, S. Durand and A. Buleon, *Carbohydr. Polym.*, 1999, **38**, 361–370.

20 D. R. Adawiyah, T. Sasaki and K. Kohyama, *Carbohydr. Polym.*, 2013, **92**, 2306–2313.

21 A. G. Maaruf, Y. B. Che Man, B. A. Asbi, A. H. Junainah and J. F. Kennedy, *Carbohydr. Polym.*, 2001, **46**, 331–337.

22 S. Mali, L. S. Sakanaka, F. Yamashita and M. V. E. Grosmann, *Carbohydr. Polym.*, 2005, **60**, 283–289.

23 N. Zhang, H. Liu, L. Yu, X. Liu, L. Zhang, L. Chen and R. Shanks, *Carbohydr. Polym.*, 2013, **92**, 455–461.

24 (a) G. A. Di Lullo, S. M. Sweeney, J. Korkko, L. Ala-Kokko and J. D. San Antonio, *J. Biol. Chem.*, 2002, **277**, 4223–4231; (b) A. Mandal, S. Panigrahi and C. Zhang, *Biol. Eng.*, 2010, **2**, 63–88.

25 J. A. M. Ramshaw, J. A. Werkmeister and V. Glattauer, *Biotechnol. Genet. Eng. Rev.*, 1995, **13**, 335–382.

26 F. Pati, P. Datta, B. Adhikari, S. Dhara, K. Ghosh and P. K. D Mohapatra, *J. Biomed. Mater. Res. Part A*, 2012, **100A**, 1068–1079.

27 A. Mandal, S. Sekar, M. Kanagavel, N. Chandrasekaran, A. Mukherjee and T.P. Sastry, *Biochim. Biophys. Acta*, 2013, **1830**, 4628–4633.

28 Y. Y. Peng, V. Glattauer, J. A. M. Ramshaw and J. A. Werkmeister, *J. Biomed. Mater. Res. A*, 2010, **93**, 1235–1244.

29 M. H. Uriarte-Montoya, J. L. Arias-Moscoso, M. Plascencia-Jatomea, H. Santacruz-Ortega, O. Rouzaud-Sa´ndez, J. L. Cardenas-Lopez, E. Marquez-Rios and J. M. Ezquerra-Brauer, *Bioresour. Technol.*, 2010, **101**, 4212–4219.

30 S. Kimura, Y. Takema and M. Kubota, *J. Biol. Chem.*, 1981, **256**, 13230–13234.

31 S. Kimura, Y. Omura, M. Ishida and H. Shirai, *Comp. Biochem. Physiol. B*, 1993, **104**, 663–668.

32 C. Rose, M. Kumar and A. B. Mandal, *Biochem. J.*, 1988, **249**, 127 133.

33 C. Rose and A. B. Mandal, *Int. J. Biol. Macromol.*, 1996, **18**, 41–53.

34 S. Kim and E. Mendis, *Food Res. Inter.*, 2006, **39**, 383–393.

35 F. Pati, B. Adhikari and S. Dhara, *Bioresour. Technol.*, 2010, **101**, 3737–3742.

36 F. Pati, P. Datta, B. Adhikari, S. Dhara, K. Ghosh, P. K. D. Mohapatra, *J. Biomed. Mater. Res. Part A*, 2012, **100A**, 1068–1079.

37 T. Ikoma, H. Kobayashi, J. Tanaka, D. Walsh and S. Mann, *Int. J. Biol. Macromol.*, 2003, **32**, 199–204.

38 E. Song, Y. S. Kim, T. Chun, H. J. Byun and Y. M. Lee, *Biomaterials*, 2006, **27**, 2951–2961.

39 P. Jitendra, A. M. Rajam, T. Kalaivani, A. B. Mandal and C. Rose, *ACS Appl. Mater. Interfaces*, 2013, **5**, 7291–7298.

40 S. Sankar, S. Sekar, R. Mohan, R. Sunita, J. Sundaraseelan and T. P. Sastry, *Int. J. Biol. Macromol.*, 2008, **42**, 6–9.

41 U. K. Laemmli, *Nature*, 1970, **227**, 680–685.

42 CLSI/NCCLS, Methods for dilution antimicrobial susceptibility tests for bacteria that grow aerobically; Approved Standard, 7th edn., 2006.

43 P. K. Khanna, N. Singh, S. Charan, V. V. V. S. Subbarao, R. Gokhale and U. P. Mulik, *Mater. Chem. Phys.*, 2005, **93**, 117–121.

44 A. Mandal, S. Sekar, N. Chandrasekaran, A. Mukherjee and T. P. Sastry, *Proceedings of the Institution of Mechanical Engineers, Part H: Journal of Engineering in Medicine*, 2013, **227**, 1224–1236**.**

45 S. Chandra, K. C. Barick and D. Bahadur, *Adv. Drug Deliv. Rev.*, 2011, **63**, 1267–1281.

46 Y. N. Rao, D. Banerjee, A. Datta, S. K. Das, R. Guin and A. Saha, *Radiat. Phys. Chem.*, 2010, **79**, 1240–1246.

47 S. Monti, E. Bramanti, V. D. Porta, M. Onor, A. D'Ulivoa and V. Barone, *Phys. Chem. Chem. Phys.*, 2013, **15**, 14736–14747.

48 A. George and A. Veis, *Biochemistry*, 1991, **30**, 2372–2377.

49 J. M. Sanchez-Ruiz, J. L. Lopez-Lacomba, M. Cortijo and P. L. Mateo, *Biochemistry*, 1988, **27**, 1648–1652.

50 K. M. Seeni Meera, R. M. Sankar, A. Murali, S. N. Jaisankar and A. B. Mandal, *Colloids Surf. B: Biointer.*, 2012, **90**, 204–210.

51 N. Sultana and M. Wang, International Conference on Biomedical Engineering and Technology IPCBEE, 2011, **11**, 24–28.

52 W. Hsieh, C. Chang and S. Lin, *Colloids Surf B: Biointer.* 2007, **57**, 250–255.

53 K. Shimizu, A. Ito and H. Honda, *J. Biomed. Mater. Res. B Appl. Biomater.*, 2005, **77**, 265–272.

54 M. P. Devi, M. Sekar, M. Chamundeswari, A. Moorthy, G. Krithiga, N. S. Murugan and T. P. Sastry, *Bull. Mater. Sci.*, 2012, **35**, 1157–1163.

55 V. Ramnath, S. Sekar, S. Sankar, C. Sankaranarayanan and T. P. Sastry, *J. Mater. Sci: Mater. Med.*, 2012, **23**, 3083–3095.

56 P. Arockianathan, S. Sekar, S. Sankar, B. Kumaran and T. P. Sastry, *Int. J. Biol. Macromol.*, 2012, **50**, 939–946.

57 A. Mandal, R. S. G. Krishnan, S. Thennarasu, S. Panigrahi and A. B. Mandal, *Colloids Surf. B: Biointerfaces*, 2010, **79**, 136-141.

58 B. Naskar, S. Ghosh and S. P. Moulik, Langmuir, 2012, **28**, 7134-7146.

59 A. B. Mandal, D. V. Ramesh and S. C. Dhar, *Eur. J. Biochem.*, 1987, **169**, 617-628.

60 B. Chudasama, A. K. Vala, N. Andhariya, R. V. Mehta and R. V. Upadhyay, *J. Nanopart. Res.*, 2010, **12**, 1677-1685.

61 J. R. Morones, J. L. Elechiguerra, A. Camacho, K. Holt, J. B. Kouri, J. T. Ramirez and M. J. Yacaman, *Nanotechnol.*, 2005, **16**, 2346–2353.

62 K. H. L. Kwan, X. Liu, M. K. T. To, K. W. K. Yeung, C. Ho and K. K. Y. Wong, *Nanomedicine: NBM*, 2011, **7**, 497–504.